HIGH-POWER EXPERIMENTAL STUDY ON A COMPACT C-BAND SPHERICAL PULSE COMPRESSOR

Y. Wei*[1], D. Alesini[4], Z. Cao[1], L. Faillace[4], G. Feng[1], P. Huang[1],
Z. Huang[1], S. Jiang[2,3], X. Liu[2,3], L. Sun[1], H. Zhang[2,3], Y. Zhang[1]
[1]University of Science and Technology of China, Hefei, China
[2]Institute of High Energy Physics, Chinese Academy of Sciences, Beijing, China
[3]Spallation Neutron Source Science Center, Dongguan, China
[4]INFN Frascati National Laboratories, Frascati, Rome, Italy

Abstract

In order to enhance the accelerating gradient of the 1-meter C-band Traveling-wave accelerating structure, as well as meet the physics requirements on the linear injector of the proposed Jinhua light source (JHLS) project, a compact C-band spherical pulse compressor was developed to boost the output power from klystron. This pulse compressor excites TE_{114} modes inside the spherical cavity by coupling power via a compact polarized coupler. In the preliminary high-power tests, an input pulse of 8.7 MW, 2.6 µs was compressed to 53.9 MW,400 ns output pulse through this pulse compressor, thereby enabling an average power gain of 4.2. Amplitude modulation (AM) was utilized to generate a flat-top output pulse. After modulation, an average power gain of 3.78 with a full-width at half-maximum (FWHM) pulse duration of 280 ns was achieved.

INTRODUCTION

The proposed Jinhua Light Source (JHLS) project is being developed by the National Synchrotron Radiation Laboratory (NSRL) at University of Science and Technology of China (USTC). Its linear injector consists of a C-band unit and a S-band unit. In the C-band unit, a C-band klystron is utilized to deliver 2.5-µs duration pulses with a peak power of 40 MW to two C-band accelerating structures, achieving an average gradient of 40 MV/m.

To date, a 1-meter C-band accelerating structure with a filling time of 253 ns has been developed [1]. In order to satisfy the requirements of the JHLS physics and high-power tests on our C-band accelerating structure, a compact C-band spherical pulse compressor based on dual-mode polarized coupler and the TE_{114} mode storage cavity has been developed, as reported in [2]. Firstly, this pulse compressor should be sufficient for filling up the whole C-band accelerating structure. Additionally, it exhibits a trade-off between the power gain and the compression efficiency. The basic parameters of this C-band unit are listed in Table 1.

The rest of this paper is organized as follows. Section II briefly describes the RF design of this C-band pulse compressor, Section III presents the cold-test results after tuning, Section IV presents the high-power tests as well as the flattop pulse experiment. Section V summarizes this paper.

* wylong@ustc.edu.cn

Table 1: Basic Parameters of the C-Band RF Unit

Parameter	Value	Unit
Operating frequency /f	5.712	GHz
Klystron power /P_{in}	40	MW
Repetition rate	60	Hz
Pulse width (uncompressed)/t_1	2.5	µs
Pulse width (compressed) /$t_2 - t_1$	300	ns
Output power /P_{out}	≥150	MW

RF DESIGN

In this C-band pulse compressor, the sphere cavity is chosen to operate at TE_{114} modes because of the higher quality factor and the available cavity size. The dual-mode polarized coupler is designed to convert TE_{10} mode at the rectangular waveguide into orthogonally polarized TE_{11} modes at the circular waveguide. This coupler is optimized to achieve the impedance matching so that the RF power can be transmitted smoothly into the storage cavity with negligible reflections. Meanwhile, the emitted power will flow to the other waveguide port instead of returning back to klystron. For more detailed information, see [2].

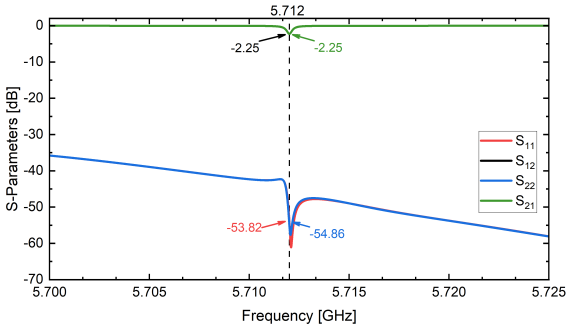

Figure 1: S-parameters of the whole C-band spherical pulse compressor.

In summary, this C-band spherical pulse compressor is designed to realize an optimized average power gain of 4.49 with a high coupling coefficient of 8. The corresponding efficiency is 54.2%. The simulated S-parameters of the whole C-band spherical pulse compressor are shown in Fig. 1.

Figure 2 shows the simulated electric field, magnetic field, and modified Poynting vector S_c [3] on the surface of the pulse compressor at an input power of 1 W from port

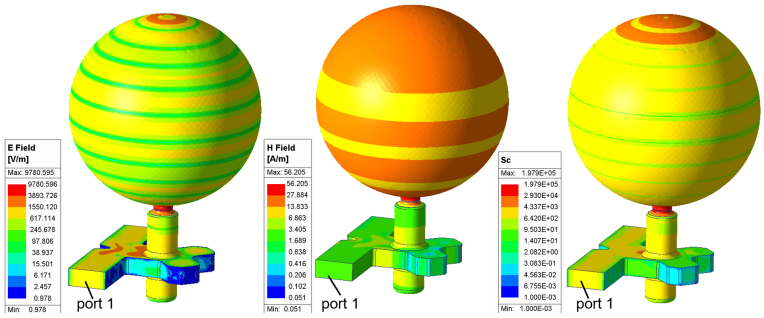

Figure 2: (a) Electric field, (b) magnetic field and (c) S_c on the surface of the C-band spherical pulse compressor.

1. The peak fields are examined to remain below the theoretical thresholds of the C-band structure to avoid a high RF breakdown rate (BDR). The pulsed heating effects of an arbitrary pulse can be calculated as follows [4]:

$$T(t) = \frac{1}{\sqrt{\pi k \rho c_\varepsilon}} \int_0^t \frac{R_s |H(t')|^2}{2\sqrt{t-t'}} dt' \quad (1)$$

where R_s is the surface resistance, k is the thermal conductivity, c_ϵ is the heat capacity. $|H(t)|$ is the maximum surface magnetic field. The corresponding peak temperature rise caused by the pulsed heating is calculated to be 46 K at an input power of 40 MW and a pulse width of 2.5 µs, which is below the C-band temperature rise threshold. Therefore, this C-band pulse compressor can be speculated to operate in the high-power tests with a low BDR.

COLD-TEST AND TUNING

In this section, we briefly introduce the cold-test measurement and tuning process. This C-band spherical pulse compressor was fabricated and then cold-tested through the vector network analyzer. The tuning process was employed to correct the asymmetry of the polarized modes as well as compensate the frequency deviation. Figure 3(a) illustrates the measured S-parameters before tuning, the coupling coefficient before tuning is only calculated to be 3.86 . Equations (2) and (3) can be utilized to re-construct the polarized modes from the S-parameters [5]:

$$\Gamma_1, \Gamma_2 = S_{12}/j \pm \sqrt{-S_{11}S_{22}} \quad (2)$$

$$\theta = \arg(-S_{22}/S_{11})/4 \quad (3)$$

It can be seen from Fig. 3 (b) that there is a frequency separation of the polarized TE modes, which is caused by the roundness error during fabrication. After tuning, the operating frequency is tuned to 5.712 GHz while the TE modes separation has been compensated, as shown in Fig. 4. The measured $S_{21} = -2.29$ dB , $S_{11} < -30$ dB. The unloaded quality factor and coupling coefficient are calculated to be 1.26×10^5 and 7.65, respectively.

The resonant peak (Fig. 4) which exhibits a 2.73 MHz separation from the operating modes is speculated to be TE_{014} degenerated mode. And it has negligible effect on the RF performance due to the large deviation.

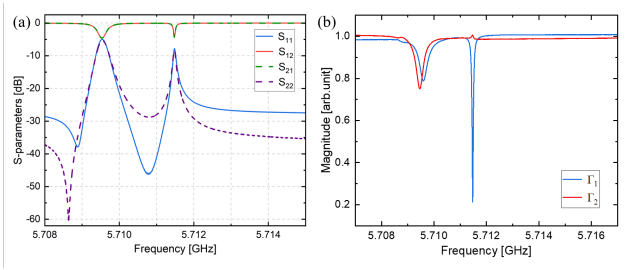

Figure 3: (a) S-parameters and (b) polarized modes before tuning.

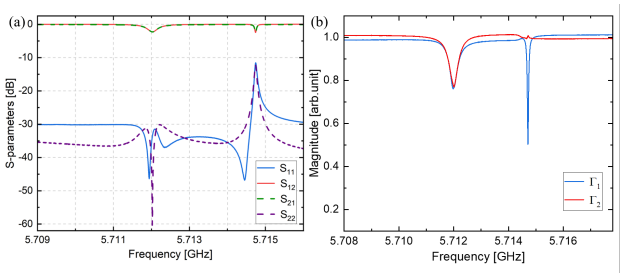

Figure 4: (a) S-parameters and (b) polarized modes after tuning.

HIGH-POWER TEST

After tuning, this C-band pulse compressor was high-power tested at the test platform of the Spallation Neutron Source Science Center, in Dongguan. hows the test picture.

This prototype was powered by a 40-MW C-band klystron with a repetition rate of 10 Hz, as shown in Fig. 5. The low level radio-frequency control system (LLRF) was utilized to reverse the input pulse phase as well as quantify

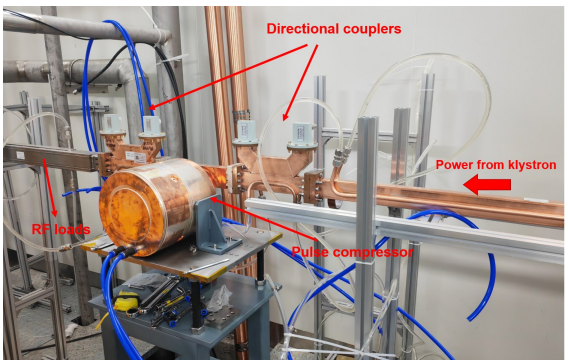

Figure 5: High-power test picture.

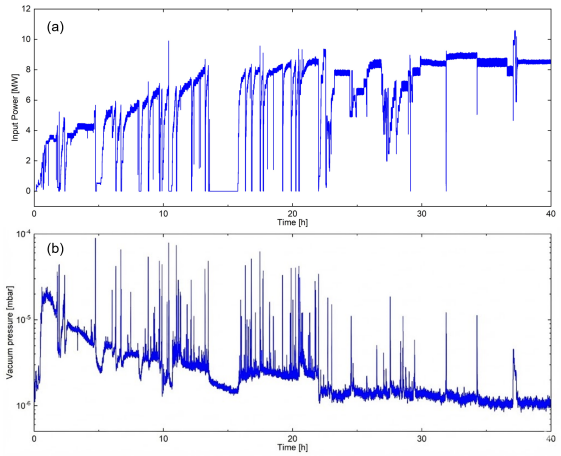

Figure 6: High-power test history of the C-band spehrical pulse compressor.

the input and output power amplitude. After conditioning with 15 hours at a repetition rate of 10 Hz, an input power of 8.7 MW from the klystron was achieved, being resulted in an output power of 53.9 MW with a pulse width of 400 ns for this pulse compressor. The average power gain was 4.2. Because of the other assignments on the test platform and the maximum absorbing capacity of RF load is limited to 60 MW, the conditioning input power was terminated at 8.7 MW.Nevertheless, the further high-power conditioning is anticipated to achieve output power exceeding 150 MW.

The conditioning history of this pulse compressor prototype are shown in Fig. 6. During an 10-hour operation at the maximum power level, a breakdown rate of 1.85×10^{-5} breakdown per pulse (bpp) was realized. A primary contributor to the increased BDR was the insufficient vacuum environment. However, it can be speculated that this pulse compressor would operate with excellent RF performance in better vacuum environment.

Furthermore, we have employed the amplitude modulation (AM) experiment to generate the flattop output pulse via the LLRF system. In AM, the input power level was 8.7 MW, a linear modulation was utilized to compensated the decaying output waveform. Through adjusting the input pulse amplitude $V_0 = -0.05$ and the increase rate $i = 80$, a quasi-flattop output pulse can be achieved. Figure 7 illustrates the input and flattop output waveform in AM experiment. The flattop width (full width of 0.9 maximum) has changed to 280 ns, including a rise time of 20 ns caused by the modulator. In this case, the output power was 32.9 MW and the average power gain was 3.78. Furthermore, AM method can be improved through manually adjusting the amplitude of each sample point with a finer step.

CONCLUSION

A compact C-band spherical pulse compressor has been developed in this paper. It utilizes the dual-mode polarized coupler to excite TE_{114} operating modes, realizing an average power gain of 4.49. The cold-test results have shown a good agreement with the simulated values. In the high-power test, an input pulse of 8.7 MW with a pulse width of 2.6 µs was compressed into a 400 ns output pulse with a peak power of 53.9 MW, yield an average power gain of 4.2. The AM method was also employed to generate a quasi-flattop output pulse with an average power gain of 3.78.

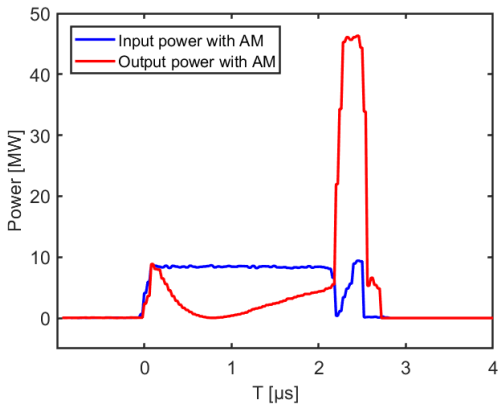

Figure 7: Input and output power waveforms with AM.

ACKNOWLEDGMENT

This work is supported by the "Hundred Talents Program" of the Chinese Academy of Sciences (Grant No. KJ2310007003), the Fundamental Research Funds for the Central Universities (Grant No. WK2310000114), Chinese Academy of Sciences President's International Fellowship Initiative (Grant No. 2025PD0102), National Key Research and Development Program of China (Grant No. 2024YFA1612200) and the 12th Research Institute of China Electronics Technology Group Corporation (Grant No. K2301287).

REFERENCES

[1] Y. Zhang *et al.*, "Design, Fabrication, and Cold Test of a High-Efficiency C-Band Traveling-Wave Accelerating Structure", *IEEE Trans. Nucl. Sci.*, vol. 72, no. 8, pp. 2868–2876, Aug. 2025. doi:10.1109/TNS.2025.3591648

[2] Z. Cao *et al.*, "Design, Fabrication, and Tests of a C-Band Spherical Pulse Compressor", *IEEE Trans. Nucl. Sci.*, vol. 72, no. 11, pp. 3452–3461, Nov. 2025. doi:10.1109/TNS.2025.3616219

[3] A. Grudiev , S. Calatroni, and W. Wuensch, "New local field quantity describing the high gradient limit of accelerating structures", *Phys. Rev. ST Accel. Beams*, vol. 12, no. 10, p. 102001, Oct. 2009. doi:10.1103/PhysRevSTAB.12.102001

[4] X. Wu and A. Grudiev, "Novel open cavity design for rotating mode rf pulse compressors", *Phys. Rev. Accel. Beams*, vol. 24, no. 11, p. 112001, Nov. 2021. doi:10.1103/PhysRevAccelBeams.24.112001

[5] X. Lin *et al.*, "X-band two-stage rf pulse compression system with correction cavity chain", *Phys. Rev. Accel. Beams*, vol. 25, no. 12, p. 120401, Dec. 2022. doi:10.1103/PhysRevAccelBeams.25.120401